

Positive Numerical Splitting Method for the Hull and White 2D Black-Scholes Equation

T. Chernogorova, R. Valkov
Faculty of Mathematics and Informatics,
University of Sofia, 1164 Sofia, Bulgaria,
{chernogorova,rvalkov}@fmi.uni-sofia.bg

January 13, 2023

Abstract

In this paper we present a locally one-dimensional (LOD) splitting method to solve numerically the two-dimensional Black-Scholes equation, arising in the Hull and White model for pricing European options with stochastic volatility, characterized by the presence of a mixed derivative term. The parabolic equation degenerates on the boundary $x = 0$ and we apply a fitted finite-volume difference scheme in order to resolve the degeneration. Discrete maximum principle is proved and therefore our method is positivity-preserving. Numerical experiments illustrate the efficiency of our difference scheme.

Keywords. Hull and White, mixed derivative, operator splitting, fitted finite volume method, boundary corrections, M-matrix

1 Introduction

The rapid development of computational finance in the past decades has been initiated by the derivation of the Black-Scholes model for pricing European options [3]. Their assumptions on the stochastic process, followed by the stock price, are rather unrealistic and nowadays there are many generalizations of the basic Black-Scholes model, resulting in linear and nonlinear multidimensional problems. Hull and White [15] proposed a model for valuing an option with a stochastic volatility of the price of the underlying stock that constitutes an important two-dimensional extension to the celebrated, one-dimensional, Black-Scholes PDE. Since no closed-form analytical formulas have been derived for any but the simplest cases of multidimensional problems in mathematical finance computationally efficient and accurate numerical methods are needed for the general case of time- and path-dependent market parameters. Over the years, various numerical techniques have been developed [6, 11, 12, 16, 27].

This paper is focused on the numerical solution of the Black-Scholes equation in stochastic volatility models. The features of this parabolic, two-dimensional

convection-reaction-diffusion problem is the presence of a *mixed spatial derivative term*, stemming from the correlation between the two underlying stochastic processes for the asset price and its variance, and *degeneration* of the parabolic equation on a part of the domain boundary. Existence of solutions to degenerate parabolic PDEs such as the Hull and White model does not follow from classical theory [21] and additional analysis is needed [10, 13].

Semi-discretization in space of such PDEs by finite-difference schemes gives rise to large systems of stiff ODEs. Standard implicit one-stepping schemes are not suitable for the efficient numerical solution of these large systems and by this reason splitting methods are designed [14].

A stable and convergent two-dimensional finite volume element method is designed by Huang et al. [12]. We adopt a different approach, executing operator splitting and temporal discretization before we handle the degeneration of the problem in space by using the fitted finite-volume method, proposed by Wang [23] and further developed in [2, 5]. The attractive features of our numerical method are computational efficiency and positivity (short for non-negativity) of the numerical solution.

In Section 2 we formulate the differential problem and present a brief analysis for existence and uniqueness of a weak solution as well as the weak maximum principle. Section 3 contains the full description of the splitting method. In Section 4 we perform numerical tests with the splitting scheme and we analyze experimentally the global error in discrete norms.

2 The Differential Problem

The price u of an European option with stochastic volatility \sqrt{y} and expiry date T satisfies the following second-order partial differential equation [15]

$$-\frac{\partial u}{\partial t} - \frac{1}{2} \left[x^2 y \frac{\partial^2 u}{\partial x^2} + 2\rho \xi x y^{3/2} \frac{\partial^2 u}{\partial x \partial y} + \xi^2 y^2 \frac{\partial^2 u}{\partial y^2} \right] - r x \frac{\partial u}{\partial x} - \mu y \frac{\partial u}{\partial y} + r u = 0, \quad (1)$$

for $(x, y, t) \in (0, X) \times (\zeta, Y) \times (0, T) =: \Omega \times (0, T)$ with the final (*payoff*) and Dirichlet boundary conditions on the boundary $\partial\Omega$ of Ω

$$u(x, y, T) = u_T(x, y), \quad (x, y) \in \Omega, \quad (2)$$

$$u(x, y, t) = u_D(x, y, t), \quad (x, y, t) \in \partial\Omega \times (0, T), \quad (3)$$

where x denotes the price of the underlying stock, ξ and μ are constants from the stochastic process, governing the variance y , ρ is the instantaneous correlation between x and y and ζ , X , Y and T are positive constants, defining the solution domain.

In the subsequent considerations we assume that $u_D(x, y, t) = 0$, i.e. we subtract a known function, satisfying the boundary condition in (3), from both sides of (1) so that a nonzero term g is introduced in the right-hand side of (1).

As mentioned in [15], ρ can not take negative value, $\rho \in [0, 1)$. In this paper we assume that $\rho \in [0, 1)$ is a constant. It is also reasonable to assume

that $y \geq \zeta$ for a (small) positive constant ζ since the $y = 0$ is trivial as the volatility of the stock is zero in the market and therefore the price of the option is deterministic.

Introducing a new variable $\tilde{u} = \exp(\beta t)u$, where $\beta > 0$ is an arbitrary constant, (1) is rewritten in the following general non-homogeneous equation after a change $\tilde{t} = T - t$ (back to the previous notations of the time variable and the solution):

$$\frac{\partial u}{\partial t} - \frac{1}{2} \left[x^2 y \frac{\partial^2 u}{\partial x^2} + 2\rho \xi x y^{3/2} \frac{\partial^2 u}{\partial x \partial y} + \xi^2 y^2 \frac{\partial^2 u}{\partial y^2} \right] - r x \frac{\partial u}{\partial x} - \mu y \frac{\partial u}{\partial y} + (r + \beta)u = g, \quad (4)$$

with the homogeneous boundary condition on $\partial\Omega$.

2.1 Well-posedness and maximum principle

The well-posedness considerations in this subsection are presented by Huang et al. [13]. We further extent their variational analysis by deriving the weak maximum principle for equation (4), written in the following divergence form

$$\frac{\partial u}{\partial t} - \nabla \cdot (k(u)) + cu = g, \quad (5)$$

$k(u) = A\nabla u + \mathbf{b}u$ is the flux, $\mathbf{b} = (rx - \frac{3}{4}\rho y^{1/2}\xi x - yx, \mu y - \frac{1}{2}\rho\xi y^{3/2} - \xi^2 y)^T$,

$$A = \begin{pmatrix} a_{11} & a_{12} \\ a_{21} & a_{22} \end{pmatrix} = \begin{pmatrix} \frac{1}{2}yx^2 & \frac{1}{2}\rho y^{3/2}\xi x \\ \frac{1}{2}\rho y^{3/2}\xi x & \frac{1}{2}\xi^2 y^2 \end{pmatrix}, \quad (6)$$

$$c = \beta + 2r - \frac{3}{4}\rho y^{1/2}\xi - y + \mu - \frac{3}{4}\rho y^{1/2}\xi - \xi^2.$$

Let $L^p(\Omega)$ denote the space of all p -integrable functions on Ω for $p \geq 1$. For $p = 2$ the inner product on $L^2(\Omega)$ is given by $(u, v) := \int_{\Omega} uv d\Omega$ with the norm $\|v\|_0^2 := \int_{\Omega} v^2 d\Omega$. The standard symbols for inner products and Sobolev spaces are used without explicitly defining them, i.e. we use $\|w\|_{1,\infty,S}$ to denote the sup-norm of ∇w on the (open) set S .

To handle the degeneracy in the Black-Scholes equation the weighted inner product on $(L^2(\Omega))^2$ is introduced by $(\mathbf{u}, \mathbf{v})_{\tilde{\omega}} := \int_{\Omega} (yx^2 u_1 v_1 + y^2 u_2 v_2) d\Omega$ for any $\mathbf{u} = (u_1, u_2)^T$ and $\mathbf{v} = (v_1, v_2)^T \in (L^2(\Omega))^2$. The corresponding weighted L^2 -norm is

$$\|\mathbf{v}\|_{0,\tilde{\omega}} := \sqrt{(\mathbf{v}, \mathbf{v})_{\tilde{\omega}}} = \left(\int_{\Omega} (yx^2 v_1^2 + y^2 v_2^2) d\Omega \right)^{1/2}.$$

The space of all weighted square-integrable functions is defined as

$$\mathbf{L}_{\tilde{\omega}}^2(\Omega) := \left\{ \mathbf{v} \in (L^2(\Omega))^2 : \|\mathbf{v}\|_{0,\tilde{\omega}} < \infty \right\}.$$

The pair $(\mathbf{L}_{\tilde{\omega}}^2(\Omega), (\cdot, \cdot)_{\tilde{\omega}})$ is a Hilbert space (cf., for example, [17]) and further the weighted Sobolev space $H_{\tilde{\omega}}^1(\Omega)$ is given by

$$H_{\tilde{\omega}}^1(\Omega) = \{ v : v \in L^2(\Omega), \nabla v \in \mathbf{L}_{\tilde{\omega}}^2(\Omega) \}$$

with the energy norm $\|v\|_{1,\hat{\omega}}^2 = |v|_{1,\hat{\omega}}^2 + \|v\|_0^2$ for any $v \in H_{\hat{\omega}}^1(\Omega)$, $|v|_{1,\hat{\omega}}^2 = \|\nabla v\|_{0,\hat{\omega}}^2$.

As discussed in [13] no boundary condition at $x = 0$ can be imposed on that part of the boundary because of the degeneracy of the equation at this part of boundary, i.e. a solution to Problem 1 can not take a trace at $x = 0$ and this is also true for the discrete problem in Section 3. A detailed discussion on this can be found in [1, 21, 26]. Nevertheless when we solve the problem numerically, we may simply choose a particular solution with a homogeneous trace at $x = 0$.

The boundary segments of Ω with $x = X$, $y = \zeta$ and $y = Y$ are denoted by $\partial\Omega_D = \{(x, y) \in \partial\Omega : x \neq 0\}$ so that we introduce

$$H_{0,\hat{\omega}}^1(\Omega) = \{v : v \in H_{\hat{\omega}}^1(\Omega) \text{ and } v|_{\partial\Omega_D} = 0\}.$$

We define the following variational problem, corresponding to (5) and (2),(3), by this Sobolev space.

Problem 1 Find $u(t) \in H_{0,\hat{\omega}}^1(\Omega)$, satisfying the initial condition (2) such that for all $v \in H_{0,\hat{\omega}}^1(\Omega)$

$$\left(\frac{\partial u(t)}{\partial t}, v \right) + \mathbf{B}(u(t), v; t) = (g, v) \text{ a.e. in } (0, T),$$

where

$$\mathbf{B}(u(t), v; t) = (A\nabla u + \underline{b}u, \nabla v) + (cu, v)$$

is a bilinear form and A , \underline{b} and c are defined in (5) and (6).

Theorem 1 [13] The bilinear form $\mathbf{B}(\cdot, \cdot)$ is coercive in $H_{0,\hat{\omega}}^1(\Omega)$

$$\mathbf{B}(v, v; t) \geq C\|v\|_{1,\hat{\omega}}^2,$$

where C denotes a (generic) positive constant, independent of v and continuous in $H_{0,\hat{\omega}}^1(\Omega)$

$$\mathbf{B}(v, w; t) \leq M\|v\|_{1,\hat{\omega}}\|w\|_{1,\hat{\omega}}.$$

There exists an unique solution of Problem 1.

We are now in position to formulate the following theorem.

Theorem 2 Let $u(x, y, t) \in H_{0,\hat{\omega}}^1(\Omega)$ is a solution of (5). If $u_T(x, y) \geq 0$ and $g(x, y, t) \geq 0$ then $u(x, y, t) \geq 0$ a.e. in $Q_T := \Omega \times (0, T)$, $T > 0$.

Proof 1 For a function $u(x, y, t) \in H_{0,\hat{\omega}}^1(\Omega)$ we denote the positive and negative parts of u respectively by u^+ and u^- . That is, $u = u^+ + u^-$, $u^+ \geq 0$ and $u^- \leq 0$. By [9] we have that

$$Du^+ = \begin{cases} Du, & \text{if } u > 0, \\ 0, & \text{if } u \leq 0, \end{cases} \quad Du^- = \begin{cases} Du, & \text{if } u < 0, \\ 0, & \text{if } u \geq 0, \end{cases}$$

where D denotes derivative in classical sense. It follows that, for any indices i, j

$$u^+u^- = D_i u^+ D_j u^- = D_i u^+ u^- = u^+ D_i u^- = 0 \text{ a.e. in } \Omega.$$

We consider the weak form of (4) in Q_t

$$\int_{Q_t} \int \left(\frac{\partial u}{\partial t} - \nabla \cdot (k(u)) + cu \right) v d\Omega dt = \int_{Q_t} \int g v d\Omega dt.$$

Therefore we have

$$\begin{aligned} & \int_{\Omega} u v d\Omega - \int_{\Omega} u(x, 0) v(x, 0) d\Omega - \int_{Q_t} \int u \frac{\partial v}{\partial t} d\Omega dt - \int_{Q_t} \int g v d\Omega dt \\ & + \int_{Q_t} \int (A \nabla u + \underline{b} u) \cdot \nabla v + c u v d\Omega dt = \int_0^t \int_{d\Omega} (A \nabla u + \underline{b} u) v \cdot \bar{\mathbf{n}} d\sigma dt. \end{aligned} \quad (7)$$

Using Steklov average and taking to the limit [18] we formally take $v = -u^- \geq 0$ in (7) to obtain

$$\begin{aligned} & -\frac{1}{2} \int_{\Omega} (u^-(x, t))^2 d\Omega + \frac{1}{2} \int_{\Omega} (u^-(x, 0))^2 d\Omega \\ & - \int_0^t B(u^-, u^-; t) dt = \int_0^t \int_{\partial\Omega} (A \nabla u + \underline{b} u) u^- \cdot \bar{\mathbf{n}} d\sigma dt - \int_{Q_t} \int g u^- d\Omega dt. \end{aligned}$$

Since $u_T(x, y) \geq 0$, $g(x, y, t) \geq 0$ we have $u^-(x, y, 0) = u^-(x, y, t) |_{\partial\Omega} \equiv 0$ and

$$-\frac{1}{2} \int_{\Omega} (u^-(x, t))^2 d\Omega - \int_0^t B(u^-, u^-; t) dt = - \int_{Q_t} \int g u^- d\Omega dt \geq 0.$$

Following the coercivity of the bilinear form $\mathbf{B}(\cdot, \cdot; t)$ we arrive at

$$\frac{1}{2} \int_{\Omega} (u^-(x, t))^2 d\Omega + C \int_0^t \|u^-\|_{1, \omega}^2 dt \leq 0. \quad (8)$$

Finally, (8) implies $\int_{\Omega} (u^-(x, t))^2 d\Omega = 0$ and therefore $u^-(x, y, t) \equiv 0$. We conclude that $u(x, y, t) \geq 0$ for a.e. $t \in (0, T)$. \square

2.2 Terminal and boundary conditions

We now discuss the terminal and boundary conditions for (1). The terminal condition is taken to be the same as the *payoff* function, determined by the nature of the option (only call option is considered for brevity). Three typical choices of payoff functions are considered [24] and these conditions are independent of y as we assume that the payoff of the option does not depend on the volatility.

The ramp payoff, corresponding to the vanilla option, is given by

$$u_T(x, y) = \max(0, x - E), \quad (x, y) \in \bar{I}_x \times \bar{I}_y, \quad (9)$$

where $E < X$ denotes the exercise price of the option, $I_x = (0, X)$ and $I_y = (0, Y)$. A second choice is the *cash-or-nothing* payoff, given by

$$u_T(x, y) = BH(0, x - E), \quad (x, y) \in \bar{I}_x \times \bar{I}_y, \quad (10)$$

where $B > 0$ is a constant and H denotes the Heaviside function. Another choice is the *bullish vertical spread* payoff, defined by

$$u_T(x, y) = \max(0, x - E_1) - \max(0, x - E_2), \quad (x, y) \in \bar{I}_x \times \bar{I}_y, \quad (11)$$

where E_1 and E_2 are two exercise prices, satisfying $E_1 < E_2$. This represents a portfolio of buying one call option with exercise price E_1 and issuing one call option with the same expiry date but a larger exercise price, E_2 .

The boundary conditions at $x = 0$ and $x = X$ are simply taken to be the extension of the terminal conditions at the points, i.e.

$$u_D(0, y, t) = u_T(0, y) = 0 \text{ and } u_D(X, y, t) = u_T(X, y). \quad (12)$$

The boundary conditions at $y = \zeta$ ($y = Y$) is the numerical solution of the standard one-dimensional Black-Scholes equation for $\xi = \mu = 0$ and the particular value $\sigma = \sqrt{\zeta}$ ($\sigma = \sqrt{Y}$), computed by the algorithm in [23].

3 LOD Additive Splitting and Full Discretization

We aim to construct a stable, positivity-preserving numerical method, applicable to (1). In Section 2 we discussed the properties of the differential problem, taking into account the degeneration at $x = 0$. From numerical methods' point of view another difficulty is the presence of a mixed derivative, whose straightforward discretization leads to violation of the discrete maximum principle and instabilities in the numerical solution.

A suitable numerical approach to multi-dimensional problems such as (1) is the application of splitting methods [14, 16]. They are labeled *economical* schemes [20] because of their efficiency, *decreasing significantly the computational costs*. For multi-dimensional PDEs these methods are often based on dimension splitting. One distinguishes two main types of splitting methods - alternating direction implicit (ADI) and the method of fractional steps. The *locally one-dimensional* (LOD) method, based on the method of fractional steps, is a specific splitting method such that all computations are effectively one-dimensional. However, in contrast with ADI methods, the intermediate stages of LOD methods are not consistent with the original problem. The first type of LOD methods were developed in the 1950s and 60s mainly by Soviet scientists [8, 20, 25], parallel to the development of ADI methods by USA scientists [19].

3.1 The Splitting Method

We start with rewriting our equation in the following conservative form

$$\begin{aligned} & \frac{\partial u}{\partial t} - \underbrace{\frac{\partial}{\partial x} \left(a_{11} \frac{\partial u}{\partial x} + \left(b_1 - \frac{\partial a_{12}}{\partial y} \right) u \right)}_{L_1 u} + c_1 u \\ & - \underbrace{\frac{\partial}{\partial y} \left(a_{22} \frac{\partial u}{\partial y} + \left(b_2 + \frac{\partial a_{21}}{\partial x} \right) u \right)}_{L_2 u} + c_2 u - \frac{\partial}{\partial y} \left((a_{12} + a_{21}) \frac{\partial u}{\partial x} \right) = g_1 + g_2, \end{aligned}$$

where a_{11} , a_{22} , $a_{12} = a_{21}$ and b_1 , b_2 are as given in (6), $c_1 + c_2 = c$ and $g_1 + g_2 = g$. Our flux-based finite volume spatial discretization benefits from the following representation

$$\frac{\partial u}{\partial t} - \frac{\partial}{\partial x} (xw(x, y, u)) + qu - \frac{\partial}{\partial y} (y\hat{w}(y, u)) + \hat{q}u - \frac{\partial}{\partial y} \left(k(x, y) \frac{\partial u}{\partial x} \right) + \beta u = g,$$

$$w(x, y, u) = 0.5xy \frac{\partial u}{\partial x} + (r - y - 1.5\rho\xi y^{1/2}) u, \quad q(y) = 1.5r - y - 1.5\rho\xi y^{1/2},$$

$$\hat{w}(y, u) = 0.5\xi^2 y \frac{\partial u}{\partial y} + (\mu - \xi^2) u, \quad \hat{q}(y) = 0.5r + \mu - \xi^2, \quad k(x, y) = \rho\xi xy^{3/2}.$$

An equidistant truncation of $[0, T] \{t_k = k\tau, k = 0, 1, \dots, K, \tau = \frac{T}{K}\}$ and a non-uniform mesh $\bar{w} = \bar{w}_x \times \bar{w}_y$ by space steps $h_i^x, i = 0, \dots, N - 1$ and $h_j^y, j = 0, \dots, M - 1$ for x and y , respectively, and a secondary mesh $x_{i\pm 1/2} = 0.5(x_{i+1} + x_i)$, $y_{j\pm 1/2} = 0.5(y_{j+1} + y_j)$, $x_{-1/2} \equiv x_0 = 0$, $x_{N+1/2} \equiv x_N = X$, $y_{-1/2} \equiv y_0 = \zeta$, $y_{M+1/2} \equiv y_M = Y$ allow us to consider the LOD additive scheme

$$\begin{aligned} u^{(1)} & \left\{ \begin{array}{l} \frac{\partial u^{(1)}}{\partial t} + L_1 u^{(1)} = g_1, \quad t_k < t \leq t_{k+1}, \\ u^{(1)}(x, y, 0) = u_T(x), \quad (x, y) \in [0, X] \times [\zeta, Y], \\ u^{(1)}(0, y, t) = u_D(0, y, t), \quad (y, t) \in [\zeta, Y] \times [0, T], \\ u^{(1)}(X, y, t) = u_D(X, y, t), \quad (y, t) \in [\zeta, Y] \times [0, T], \end{array} \right. \\ u^{(2)} & \left\{ \begin{array}{l} \frac{\partial u^{(2)}}{\partial t} + L_2 u^{(2)} = g_2, \quad t_k < t \leq t_{k+1}, k = 1, 2, \dots, K, \\ u^{(2)}(x, y, t_k) = u^{(1)}(x, y, t_{k+1}), \quad (x, y) \in [0, X] \times [\zeta, Y], \\ u^{(2)}(x, \zeta, t) = u_D(x, \zeta, t), \quad (x, t) \in (0, X] \times (0, T], \\ u^{(2)}(x, Y, t) = u_D(x, Y, t), \quad (x, t) \in (0, X] \times (0, T]. \end{array} \right. \end{aligned}$$

3.2 Analysis of time semi-discretization

The construction of our numerical scheme demands that *we begin by executing a time discretization*. We obtain semi-discrete approximations $u^k(x, y)$ to the

solution $u(x, y, t)$ of (1)-(3) at $t = t_k = k\tau$ by using the following fractional steps scheme

$$(I + \tau L_1)u^{k+1/2} = u^k + \tau g_1, \quad (13)$$

$$u^0 = u_T(x, y), \quad (14)$$

$$u^{k+1/2}(0, y) = u_D(0, y, t_{k+1}), \quad u^{k+1/2}(X, y) = u_D(X, y, t_{k+1}), \quad (15)$$

$$(I + \tau L_2)u^{k+1} = u^{k+1/2} + \tau g_2, \quad (16)$$

$$u^{k+1}(x, \zeta) = u_D(x, \zeta, t_{k+1}), \quad u^{k+1}(x, Y) = u_D(x, Y, t_{k+1}). \quad (17)$$

Prior to the next considerations we have to introduce the following weighted Sobolev space

$$H_w^1(0, X) = \{v : v \in L^2(0, X), \nabla v \in L_w^2(0, X)\},$$

taking into account the degeneration of the one-dimensional Black-Scholes equation at $x = 0$ by the weighted L^2 -norm

$$\|v\|_{0,w} := \sqrt{(v, v)_w} = \left(\int_0^X x^2 v^2 dx \right)^{1/2},$$

with the energy norm, defined by $\|v\|_{1,w}^2 = |v|_{1,w}^2 + \|v\|_0^2$ for any $v \in H_w^1(0, X)$, where $|v|_{1,w}^2 = \|\nabla v\|_{0,w}^2$. We also introduce the following subspace of $H_w^1(0, X)$

$$H_{0,w}^1(0, X) = \{v : v \in H_w^1(0, X) \text{ and } v(0) = v(X) = 0\}.$$

We need the following lemma, see Theorem A.1 by Castro and Wang [4].

Lemma 3 *Let α be any real number such that $\alpha + \frac{1}{2} > 0$. Assume that $u \in H_{loc}^1(0, X)$ and $u(X) = 0$. Then*

$$\|x^\alpha u\|_0 \leq C_{2,\alpha} \left\| x^{\alpha+1} u' \right\|_0, \quad C_{2,\alpha} = \frac{2}{1+2\alpha}.$$

Lemma 4 *Let the operator $(I + \tau L_1)^{-1}$ be such that $(I + \tau L_1)^{-1}u$ is the solution v of*

$$(I + \tau L_1)v = u, \quad v(0, y) = 0, \quad v(X, y) = 0$$

and analogously for $(I + \tau L_2)^{-1}$. Then $I + \tau L_1$ and $I + \tau L_2$ are inverse positive and satisfy the conditions

$$\|(I + \tau L_1)^{-1}\|_{L^2(\Omega)} \leq \frac{1}{1 + \tilde{C}_1 \tau}, \quad \|(I + \tau L_2)^{-1}\|_{L^2(\Omega)} \leq \frac{1}{1 + \tilde{C}_2 \tau}, \quad (18)$$

where \tilde{C}_1, \tilde{C}_2 are constants, independent of τ .

Proof 2 *We prove the result for $A_x = I + \tau L_1$ since similar considerations can be applied to the other operator. Introducing the notations $a(y) = 0.5y, b(y) = r - y - 1.5\rho\xi y^{1/2}, c(y) = 1.5r - y - 1.5\rho\xi y^{1/2} + 0.5\beta$ we derive*

$$A_x u^{k+1/2} = -\tau \frac{\partial}{\partial x} \left(x \left(a(y)x \frac{\partial u^{k+1/2}}{\partial x} + b(y)u^{k+1/2} \right) \right) + (1 + \tau c(y))u^{k+1/2} = u^k.$$

Applying integration by parts one obtains

$$\begin{aligned} \left(A_x u^{k+1/2}, u^{k+1/2} \right)_{L^2(0,X)} &= \tau \int_0^X \left(x \left(a(y)x \frac{\partial u^{k+1/2}}{\partial x} + b(y)u^{k+1/2} \right) \right) \\ &\cdot \frac{\partial u^{k+1/2}}{\partial x} dx + (1 + \tau c(y)) \left\| u^{k+1/2} \right\|_{L^2(0,X)}^2 = \int_0^X u^k u^{k+1/2} dx. \end{aligned} \quad (19)$$

By the Poincaré-Hardy inequality in Lemma 3 for $\alpha = 0$ we have

$$\begin{aligned} \left(A_x u^{k+1/2}, u^{k+1/2} \right)_{L^2(0,X)} &= C_1 \tau a(y) \left| u^{k+1/2} \right|_{H_{0,w}^1(0,X)}^2 - 0.5 \tau b(y) \\ &\cdot \left\| u^{k+1/2} \right\|_{L^2(0,X)}^2 + (1 + \tau c(y)) \left\| u^{k+1/2} \right\|_{L^2(0,X)}^2 \\ &\geq (1 + \tau(c(y) + C_1 a(y) - 0.5b(y))) \left\| u^{k+1/2} \right\|_{L^2(0,X)}^2. \end{aligned}$$

Application of the Cauchy-Schwarz inequality to the right-hand side of (19) results in

$$(1 + \tau(c(y) + C_1 a(y) - 0.5b(y))) \left\| u^{k+1/2} \right\|_{L^2(0,X)} \leq \left\| u^k \right\|_{L^2(0,X)}.$$

Since $c(y) = 1.5r - 1.5\rho\xi y^{1/2} + 0.5\beta$ and because β can be chosen arbitrary high one derives

$$c(y) + C_1 a(y) - 0.5b(y) \geq 0.25\beta = \tilde{\beta} > 0$$

and therefore

$$(1 + \tau\tilde{\beta})^2 \left\| u^{k+1/2} \right\|_{L^2(0,X)}^2 \leq \left\| u^k \right\|_{L^2(0,X)}^2.$$

Integrating by y from (ζ, Y) we get

$$(1 + \tau\tilde{\beta}) \left\| u^{k+1/2} \right\|_{L^2(\Omega)} \leq \left\| u^k \right\|_{L^2(\Omega)}. \quad (20)$$

The final estimate easily follows from (20)

$$\frac{\left\| A_x^{-1} u^k \right\|_{L^2(\Omega)}}{\left\| u^k \right\|_{L^2(\Omega)}} = \left\| A_x^{-1} \right\|_{L^2(\Omega)} \leq \frac{1}{1 + \tau\tilde{\beta}}.$$

Analogous estimate is obtained for $\left\| A_y^{-1} \right\|_{L^2(\Omega)}$, $A_y u^{k+1} = (I + \tau L_2) u^{k+1}$. \square

To prove the convergence of the semi-discretization we show it's consistency. We apply similar considerations as in Clavero et al. [7] and define the local error e_{n+1} by

$$e_{n+1} = u(x, y, t_{k+1}) - \hat{u}^{k+1}(x, y),$$

where \hat{u}^{k+1} is the result " u^{k+1} " of applying the semi-discrete scheme with $u^k = u(t_k)$, we have the following assertion.

Lemma 5 *The temporal discretization (13)-(17) yields*

$$\|e_{k+1}\|_{L_2(\Omega)} \leq C\tau^2, \quad (21)$$

where C is a constant, independent of τ .

Proof 3 *We observe that \dot{u}^{k+1} satisfies the equation*

$$(I + \tau L_1) \left((I + \tau L_2) \dot{u}^{k+1} - \tau g_2(t_{k+1}) \right) - \tau g_1(t_{k+1}) = u(t_k) + O(\tau^2).$$

On the other hand

$$\begin{aligned} u(t_k) &= u(t_{k+1}) + \tau(L_1 + L_2)u(t_{k+1}) + \int_{t_{k+1}}^t (t_k - s) \frac{\partial^2 u}{\partial t^2}(s) ds \\ -\tau g_1(t_{k+1}) - \tau g_2(t_{k+1}) &= (I + \tau L_1) \left((I + \tau L_2)u(t_{k+1}) - \tau g_2(t_{k+1}) \right) \\ &\quad - \tau g_1(t_{k+1}) + O(\tau^2). \end{aligned}$$

Thus e_{k+1} satisfies an equation of type

$$(I + \tau L_1) (I + \tau L_2) e_{k+1} = O(\tau^2) \quad (22)$$

and the estimate (21) easily follows from (22). \square

We define the global error for the semi-discretization process in the form

$$E_\tau = \sup_{k \leq \frac{T}{\tau}} \|u(t_k) - u^k\|_{L^2(\Omega)}.$$

Theorem 6 *The temporal discretization (13)-(17) is first-order convergent*

$$E_\tau \leq C\tau,$$

where C is a constant, independent of τ .

Proof 4 *The global error at the time t_k can be decomposed in the form*

$$\|u(t_k) - u^k\|_{L_2(\Omega)} \leq \|u(t_k) - \dot{u}^k\|_{L_2(\Omega)} + \|\dot{u}^k - u^k\|_{L_2(\Omega)}.$$

Taking into account

$$\dot{u}^k - u^k = (I + \tau L_2)^{-1} (I + \tau L_1)^{-1} (u(t_{k-1}) - u^{k-1})$$

and the estimates (18) and (21) we deduce

$$\|u(t_k) - u^k\|_{L_2(\Omega)} \leq C(\tau^2) + \|u(t_{k-1}) - u^{k-1}\|_{L_2(\Omega)}.$$

Finally, by recurrence we obtain

$$\|u(t_k) - u^k\|_{L_2(\Omega)} \leq C\tau. \square$$

3.3 Full Discretization

We now proceed to the derivation of the full discretization of problem (1)-(3). Equation (13) belongs to the second-order differential equations with non-negative characteristic form, see Oleinik and Radkevich [21]. At the boundary $x = 0$ it degenerates to

$$(1 + 0.5\tau(r + \beta))u^{k+1/2}(0, y) = u^k(0, y) + \tau g_1(0, y, t^{k+1}).$$

The numerical solution is influenced by the degeneration in the vicinity of $x = 0$, resulting in violation of the discrete maximum principle and instabilities when using standard finite difference approximations. Wang [23] proposed a finite volume element method, resolving the *degeneracy*, as the local flux approximation is determined by a set of two-point boundary value problems (BVPs), defined on the element edges.

We briefly describe the discussed finite volume method as we apply it to the first subproblem (13)-(15). By (13) we have

$$w(u) = 0.5xy \frac{\partial u}{\partial x} + \left(r - y - 1.5\rho\xi y^{1/2} \right) u =: \bar{a}(y)x \frac{\partial u}{\partial x} + \bar{b}(y)u,$$

where $\bar{a}(y) = 0.5y$ and $\bar{b}(y) = r - y - 1.5\rho\xi y^{1/2}$ are notations, used in the next considerations. Equation (13) can be written in the form

$$\begin{aligned} \frac{u^{k+1/2} - u^k}{\tau} &= \frac{\partial}{\partial x} \left(x \left(\bar{a}(y)x \frac{\partial u}{\partial x} + \bar{b}(y)u \right) \right) \\ &- \left(1.5r - y - 1.5\rho\xi y^{1/2} + 0.5\beta \right) u + g_1^{k+1}. \end{aligned} \quad (23)$$

Let y is fixed. Integrating equation (23) w.r.t. x in the interval $(x_{i-1/2}, x_{i+1/2})$, $i = 1, 2, \dots, N - 1$ and applying the mid-point quadrature rule to the integrals in the equation, we arrive at

$$\begin{aligned} \frac{u_i^{k+1/2} - u_i^k}{\tau} \bar{h}_i^x &= \left[x_{i+1/2} w(u^{k+1/2}) \Big|_{x_{i+1/2}} \right. \\ &\left. - x_{i-1/2} w(u^{k+1/2}) \Big|_{x_{i-1/2}} \right] - c_1(y)u_i^{k+1/2} \bar{h}_i^x + g_1^{k+1} \bar{h}_i^x, \end{aligned} \quad (24)$$

where $\bar{h}_i^x = x_{i+1/2} - x_{i-1/2}$, $u_i = u(x_i, y, t)$ and $c_1(y) = 1.5r - y - 1.5\rho\xi y^{1/2} + 0.5\beta$. In order to obtain an approximation for the flux in the node $x_{i+1/2}$, we consider the following BVP:

$$\begin{aligned} (\bar{a}_{i+1/2}(y)xv' + \bar{b}_{i+1/2}(y)v)'_x &= 0, \quad x \in I_i, \\ v(x_i) &= u_i, \quad v(x_{i+1}) = u_{i+1}. \end{aligned}$$

The solution of that problem is

$$w_{i+1/2}(u) = \bar{b}(y) \frac{x_{i+1}^{\bar{\alpha}_i(y)} u_{i+1} - x_i^{\bar{\alpha}_i(y)} u_i}{x_{i+1}^{\bar{\alpha}_i(y)} - x_i^{\bar{\alpha}_i(y)}}, \quad \bar{\alpha}_i = \frac{\bar{b}_{i+1/2}}{\bar{a}_{i+1/2}}.$$

When deriving the approximation of the flux at $x_{1/2}$, because of the degeneration, we consider the BVP with an extra degree of freedom

$$\begin{aligned} (\bar{a}(y)xv' + \bar{b}(y)v)'_x &= C_1, x \in I_0, \\ v(0) &= u_0, v(x_1) = u_1, \end{aligned}$$

and the approximation for $w_{1/2}(u)$ is $0.5 [(\bar{a}(y) + \bar{b}(y))u_1 - (\bar{a}(y) - \bar{b}(y))u_0]$.

It was first mentioned by Dyakonov [8] that the boundary conditions deteriorate the accuracy of the splitting method if the discrete equations on the boundaries differ from the equations for the inner nodes of the mesh. In [14, 25] the issue is also discussed and correction techniques are presented. We consider the following boundary corrections

$$\begin{aligned} \bar{u}_{0,j} &= u_D(0, y_j, t^{k+1}), j = 0, \dots, M, \\ \bar{u}_{N,j} &= u_D(X, y_j, t^{k+1}), j = 0, \dots, M, \\ \bar{\Lambda}_1 \bar{u}_{i,0} - \Lambda_1 u_{i,0}^k &= g_1(x_i, 0, t^{k+1}) \bar{h}_i^x, i = 1, \dots, N-1, \\ \bar{\Lambda}_1 \bar{u}_{i,M} - \Lambda_1 u_{i,M}^k &= g_1(x_i, Y, t^{k+1}) \bar{h}_i^x, i = 1, \dots, N-1, \end{aligned} \tag{25}$$

where the discrete operators $\bar{\Lambda}_1$ and Λ_1 match the presented discretization in the x -direction and \bar{u} is the numerical solution, corresponding to $u^{k+1/2}$.

Next, after substituting the obtained approximations for the flux in (24), considering the boundary conditions, we arrive at the scalar form the discrete problem for \bar{u} ,

$$\begin{aligned} B_0 \bar{u}_{0,j} + C_0 \bar{u}_{1,j} &= F_0, \\ A_1 \bar{u}_{0,j} + B_1 \bar{u}_{1,j} + C_1 \bar{u}_{2,j} &= F_1, \\ \dots & \\ A_i \bar{u}_{i-1,j} + B_i \bar{u}_{i,j} + C_i \bar{u}_{i+1,j} &= F_i, \\ A_1 \bar{u}_{N-1,j} + B_N \bar{u}_{N,j} &= F_N, \end{aligned} \tag{26}$$

for $i = 2, \dots, N-1$, where

$$\begin{aligned} B_0 &= 1, C_0 = 0, F_0 = u_D(0, y_j, t^{k+1}), \\ A_N &= 0, B_N = 1, F(N) = u_D(X, y_j, t^{k+1}), \\ A_1 &= -\frac{x_{1/2}}{2} (\bar{a}(y_j) - \bar{b}(y_j)), C_1 = -\frac{x_{3/2} \bar{b}(y_j) x_2^{\alpha(y_j)}}{x_2^{\alpha(y_j)} - x_1^{\alpha(y_j)}}, \\ B_1 &= \frac{\bar{h}_2^x}{\tau} + \frac{x_{3/2} \bar{b}(y_j) x_1^{\alpha(y_j)}}{x_2^{\alpha(y_j)} - x_1^{\alpha(y_j)}} + \frac{x_{1/2}}{2} (\bar{a}(y_j) + \bar{b}(y_j)) + \bar{h}_2^x c_1(y_j), \\ A_i &= -\frac{x_{i-1/2} \bar{b}(y_j) x_{i-1}^{\alpha(y_j)}}{x_i^{\alpha(y_j)} - x_{i-1}^{\alpha(y_j)}}, C_i = -\frac{x_{i+1/2} \bar{b}(y_j) x_{i+1}^{\alpha(y_j)}}{x_{i+1}^{\alpha(y_j)} - x_i^{\alpha(y_j)}}, \\ B_i &= \frac{\bar{h}_i^x}{\tau} + \frac{x_{i+1/2} \bar{b}(y_j) x_i^{\alpha(y_j)}}{x_{i+1}^{\alpha(y_j)} - x_i^{\alpha(y_j)}} + \frac{x_{i-1/2} \bar{b}(y_j) x_i^{\alpha(y_j)}}{x_i^{\alpha(y_j)} - x_{i-1}^{\alpha(y_j)}} + \bar{h}_i^x c_1(y_j), \\ F_1 &= \frac{\bar{h}_2^x}{\tau} + g_1(x_1, y_j, t^{k+1}) \bar{h}_i^x, F_i = \frac{\bar{h}_i^x}{\tau} + g_1(x_i, y_j, t^{k+1}) \bar{h}_i^x. \end{aligned}$$

This is a $(N + 1) \times (N + 1)$ linear system for the discrete solution \bar{u} of the problem (13)-(15), solved by the Thomas algorithm.

We continue with the discretization of the problem (16),(17). Introducing the notations

$$\hat{w}(u) = 0.5\xi^2 \frac{\partial u}{\partial y} + (\mu - \xi^2)u = \hat{a}y \frac{\partial u}{\partial x} + \hat{b}(y)u, \quad \hat{a} = 0.5\xi^2, \quad \hat{b}(y) = \mu - \xi^2$$

and integrating (16) w.r.t. y in the interval $(y_{j-1/2}, y_{j+1/2})$, we obtain

$$\begin{aligned} \frac{u_j^{k+1} - u_j^{k+1/2}}{\tau} \hbar_j^y &= \left[y_{j+1/2} \hat{w}(u^{k+1}) \Big|_{(x_i, y_{j+1/2}, t)} - y_{j-1/2} \hat{w}(u^{k+1}) \Big|_{(x_i, y_{j-1/2}, t)} \right] \\ &\quad - c_2 u_j^{k+1} \hbar_j^y + \left(k(x, y) \frac{\partial u^{k+1/2}}{\partial x} \right) \Big|_{(x_i, y_{j-1/2}, t)}^{(x_i, y_{j+1/2}, t)} + g_2(x, y, t^{k+1}) \hbar_j^y, \end{aligned}$$

where $\hbar_j^y = y_{j+1/2} - y_{j-1/2}$ and $c_2 = 0.5r + \mu - \xi^2 + 0.5\beta$.

For the expression $(k(x, y) \frac{\partial u}{\partial x}) \Big|_{(x_i, y_{j-1/2}, t)}^{(x_i, y_{j+1/2}, t)}$, $k(x, y) = \rho\xi xy^{3/2}$, we have the following approximation

$$\begin{aligned} \left(k(x, y) \frac{\partial u}{\partial x} \right) \Big|_{(x_i, y_{j-1/2}, t)}^{(x_i, y_{j+1/2}, t)} &= k(x_i, y_{j+1/2}) \frac{\partial u}{\partial x} \Big|_{(x_i, y_{j+1/2}, t)} - k(x_i, y_{j-1/2}) \\ &\quad \times \frac{\partial u}{\partial x} \Big|_{(x_i, y_{j-1/2}, t)} \approx k(x_i, y_{j+1/2}) \frac{1}{2} \left(\frac{\partial u}{\partial x} \Big|_{(x_i, y_{j+1}, t)} + \frac{\partial u}{\partial x} \Big|_{(x_i, y_j, t)} \right) \\ &\quad - k(x_i, y_{j-1/2}) \frac{1}{2} \left(\frac{\partial u}{\partial x} \Big|_{(x_i, y_j, t)} + \frac{\partial u}{\partial x} \Big|_{(x_i, y_{j-1}, t)} \right) \approx 0.25k(x_i, y_{j+1/2}) \\ &\quad \cdot \left(\frac{u_{i+1, j+1} - u_{i, j+1} + u_{i+1, j} - u_{i, j}}{\hbar_i^x} + \frac{u_{i, j+1} - u_{i-1, j+1} + u_{i, j} - u_{i-1, j}}{\hbar_{i-1}^x} \right) - \\ &\quad - 0.25k(x_i, y_{j-1/2}) \left(\frac{u_{i+1, j} - u_{i, j} + u_{i+1, j-1} - u_{i, j-1}}{\hbar_i^x} \right. \\ &\quad \left. + \frac{u_{i, j} - u_{i-1, j} + u_{i, j-1} - u_{i-1, j-1}}{\hbar_{i-1}^x} \right). \end{aligned}$$

The boundary corrections for the second sub-problem are

$$\begin{aligned} \hat{u}_{i,0} &= u_D(x_i, 0, t^{n+1}), \quad i = 0, \dots, N, \\ \hat{u}_{i,M} &= u_D(x_i, Y, t^{n+1}), \quad i = 0, \dots, N, \\ \hat{\Lambda}_2 \hat{u}_{0,j} - \Lambda_2 \bar{u}_{0,j} &= g_2(0, y_j, t^{k+1}) \hbar_j^y, \quad j = 1, \dots, M-1, \\ \hat{\Lambda}_2 \hat{u}_{N,j} - \Lambda_2 \bar{u}_{N,j} &= g_2(X, y_j, t^{k+1}) \hbar_j^y, \quad j = 1, \dots, M-1, \end{aligned} \tag{27}$$

where the discrete operators $\hat{\Lambda}_2$ and Λ_2 match the presented discretization in the y -direction and \hat{u} is the numerical solution, corresponding to u^{k+1} . Let

us note that at $x = 0$ and $x = X$ the discretization of the mixed derivative is changed respectively by forward and backward difference approximations in direction x as follows

$$\begin{aligned} \left(k(x, y) \frac{\partial u}{\partial x} \right) \Big|_{(0, y_{j-1/2}, t)}^{(0, y_{j+1/2}, t)} &\approx 0.5k(0, y_{j+1/2}) \left(\frac{u_{1,j+1} - u_{0,j+1} + u_{1,j} - u_{0,j}}{h_0^x} \right) \\ &\quad - 0.5k(0, y_{j-1/2}) \left(\frac{u_{1,j} - u_{0,j} + u_{1,j-1} - u_{0,j-1}}{h_0^x} \right), \\ \left(k(x, y) \frac{\partial u}{\partial x} \right) \Big|_{(X, y_{j-1/2}, t)}^{(X, y_{j+1/2}, t)} &\approx 0.5k(X, y_{j+1/2}) \\ &\quad \times \left(\frac{u_{N,j+1} - u_{N-1,j+1} + u_{N,j} - u_{N-1,j}}{h_{N-1}^x} \right) - 0.5k(X, y_{j-1/2}) \\ &\quad \times \left(\frac{u_{N,j} - u_{N-1,j} + u_{N,j-1} - u_{N-1,j-1}}{h_{N-1}^x} \right). \end{aligned}$$

Similarly to the problem for $u^{k+1/2}$, introducing $\hat{\alpha}_i = \frac{\hat{b}_{j+1/2}}{\hat{a}_{j+1/2}}$, we obtain

$$\hat{u}_{i,0} = u_D(x_i, \zeta, t_{k+1}),$$

$$\begin{aligned} y_{j-1/2} \frac{\hat{b}_{j-1/2} y_{j-1}^{\hat{\alpha}_{j-1}}}{y_j^{\hat{\alpha}_{j-1}} - y_{j-1}^{\hat{\alpha}_{j-1}}} \hat{u}_{i,j-1} - \left[\frac{\hat{h}_j^y}{\tau} + y_{j+1/2} \frac{\hat{b}_{j+1/2} y_j^{\hat{\alpha}_j}}{y_{j+1}^{\hat{\alpha}_j} - y_j^{\hat{\alpha}_j}} + y_{j-1/2} \frac{\hat{b}_{j-1/2} y_j^{\hat{\alpha}_{j-1}}}{y_j^{\hat{\alpha}_{j-1}} - y_{j-1}^{\hat{\alpha}_{j-1}}} \right. \\ \left. - \hat{h}_j^y \hat{c} \right] \hat{u}_{i,j} + y_{j+1/2} \frac{\hat{b}_{j+1/2} y_{j+1}^{\hat{\alpha}_j}}{y_{j+1}^{\hat{\alpha}_j} - y_j^{\hat{\alpha}_j}} \hat{u}_{i,j+1} = - \frac{\hat{h}_j^y \hat{u}_{i,j}}{\tau} - 0.25k(x_i, y_{j+1/2}) \\ \cdot \left(\frac{\hat{u}_{i+1,j+1} - \hat{u}_{i,j+1} + \hat{u}_{i+1,j} - \hat{u}_{i,j}}{h_i^x} + \frac{\hat{u}_{i,j+1} - \hat{u}_{i-1,j+1} + \hat{u}_{i,j} - \hat{u}_{i-1,j}}{h_{i-1}^x} \right) \\ + 0.25k(x_i, y_{j-1/2}) \left(\frac{\hat{u}_{i+1,j} - \hat{u}_{i,j} + \hat{u}_{i+1,j-1} - \hat{u}_{i,j-1}}{h_i^x} \right. \\ \left. + \frac{\hat{u}_{i,j} - \hat{u}_{i-1,j} + \hat{u}_{i,j-1} - \hat{u}_{i-1,j-1}}{h_{i-1}^x} \right) + g_2(x_i, y_j, t^{k+1}) \hat{h}_j^y. \end{aligned}$$

$$\hat{u}_{i,M} = u_D(x_i, Y, t_{k+1}),$$

Again, this $(M + 1) \times (M + 1)$ linear system for the discrete solution \hat{u} of the problem (16),(17) is solved by the Thomas algorithm.

3.4 Discrete Maximum Principle

Theorem 7 *The system matrices for both \bar{u} and \hat{u} are (can be reduced to) M -matrices.*

Proof 5 First, we prove the system matrix in (26) is an M-matrix. The following observation is valid

$$\frac{\bar{b}(y_j)x_{i+1}^{\alpha(y_j)}}{x_{i+1}^{\alpha(y_j)} - x_i^{\alpha(y_j)}} = \bar{a}(y_j) \frac{\alpha(y_j)}{1 - \bar{x}^{\alpha(y_j)}} > 0, \bar{x} = x_i/x_{i+1}$$

for each $i = 1, \dots, N-1$, $\bar{b}(y_j) \neq 0$, since $1 - \bar{x}^{\alpha(y_j)}$ has just the sign of $\alpha(y_j)$. It also holds true for $\bar{b}(y_j) \rightarrow 0$. Therefore $A_i < 0, i = 2, \dots, N-1$, and $C_i < 0$, (for small τ) $B_i > 0, i = 1, \dots, N-1$. We have

$$A_1 = -0.5x_{1/2}(\bar{a}(y_j) - \bar{b}(y_j)) = -0.5x_{1/2}(1.5y_j + 1.5\rho\xi y_j^{1/2} - r)$$

and it takes positive values for small y_j . Let us expel the first two rows out of the system matrix. We obtain

$$\begin{aligned} \bar{u}_{1,j} &= \frac{1}{B_1}(F_1 - A_1u_D(0, y_j, t^{k+1}) - C_1\bar{u}_{2,j}) \Rightarrow \tilde{B}_2\bar{u}_{2,j} + C_2\bar{u}_{3,j} = \tilde{F}_2, \\ \tilde{B}_2 &= B_2 - \frac{C_1}{B_1}A_2, \tilde{F}_2 = F_2 - A_2\frac{1}{B_1}(F_1 - A_1u_D(0, y_j, t^{k+1})). \end{aligned}$$

Since $B_2 = O(\frac{1}{\tau})$ and $\frac{C_1}{B_1}A_2 = O(\tau)$ \tilde{B}_2 has the same sign as B_2 for small τ . The reduced system is an M-matrix.

In addition, because F_2 is non-negative then so is \tilde{F}_2 , because $\frac{F_1}{B_1} = O(1)$. Moreover $\bar{u}_{1,j}$ is non-negative also because B_1 as well as $F_1 - A_1u_D(0, y_j, t^{k+1}) - C_1\bar{u}_{2,j}$ are positive from small τ .

By similar considerations we prove that the (reduced) system matrix for \hat{u} is an M-matrix. However, in order to ensure non-negativity of the load vector, a constraint on the temporal step $\tau = O(h_i^x h_j^y)$ should be present. \square

Non-negativity is of major importance in option-pricing since the price of an option can not take negative values. The following corollary follows from Theorem 7.

Corollary 1 For a non-negative functions $u_T(x, y)$ and $u_D(x, y, t)$ the numerical solution \hat{u} , generated by the splitting method, is also non-negative.

4 Numerical Experiments

Numerical experiments, presented in this section, illustrate the properties of the constructed method. We solve numerically various European Test Problems (TP) with different final (initial) conditions and different choices of parameters.

1. (TP1). Call option with final condition (9). Parameters: $X = 100, Y = 1, T = 1, \zeta = 0.01, r = 0.1, \rho = 0.9, \xi = 1, \mu = 0$ and $E = 57$.
2. (TP2). Call option with cash-or-nothing payoff (10). Parameters: $X = 100, Y = 0.36, T = 1, \zeta = 0.01, r = 0.1, \rho = 0.9, \xi = 1, \mu = 0, B = 1$ and $E = 57$.

3. (TP3). *A portfolio of options.* Combinations of different options have step final conditions such as the 'bullish vertical spread' payoff, defined in (11). In this example, we assume that the final condition is a 'butterfly spread' delta function, defined by

$$u_T(x, y) = \begin{cases} 1, & x \in (X_1, X_2), \\ -1, & S \in (X_2, X_3), \\ 0, & \text{otherwise,} \end{cases}$$

and the boundary conditions are assumed to be homogenous. It arises from a portfolio of three types of options with different exercise prices. Parameters: $X = 100$, $Y = 0.36$, $T = 1$, $X_1 = 40$, $X_2 = 50$, $X_3 = 60$, $\zeta = 0.01$, $r = 0.1$, $\rho = 0.9$, $\xi = 1$, $\mu = 0$, $B = 1$ and $E = 57$.

In the tables below are presented the computed C and L_2 mesh norms of the error $E = \hat{u}^K - u^K$ by the formulas

$$\|E\|_C = \max_{i,j} \|\hat{u}_{i,j}^K - u_{i,j}^K\|, \quad \|E\|_{L_2} = \sqrt{\sum_{i=0}^N l_i^x l_j^y (\hat{u}_{i,j}^K - u_{i,j}^K)^2}.$$

We also introduce the root mean square error (*RMSE*) on a specific region

$$\|E\|_{RMSE} = \sqrt{\frac{1}{N_{br}} \sum_{i,j}^{br} (\hat{u}_{i,j}^K - u_{i,j}^K)^2},$$

where N_{br} is the number of mesh points in the region we are interested in. The rate of convergence (RC) is calculated using double mesh principle

$$RC = \log_2(E^{N,M}/E^{2N,2M}), \quad E^N = \|\hat{u}^{N,M} - u^{N,M}\|,$$

where $\|\cdot\|$ is the mesh norm, $u^{N,M}$ and $\hat{u}^{N,M}$ are respectively the exact solution and the numerical solution, computed at the mesh with N and M subintervals in directions x and y respectively.

In Table 1 are presented results, regarding the spatial convergence, for an exact solution $u = x \exp(-yt)$ with $K = 4096$. We choose this function because it's features are similar to the analytic solution for $\rho = 0$, given in [15]. Let us note that when using an exact solution to test the numerical method a right-hand side arises. The following parameters are used: $X = Y = T = 1$, $\xi = 1$ and $\zeta = 0.01$. The choice of the other parameters ρ , r and μ differ as it is noted in the table. As expected, the results confirm that our difference scheme is first order convergent w.r.t. the space variables on a quasi-uniform mesh.

We compare the exact solution $u(x, y, t) = x \exp(-yt)$ with the numerical solution, generated by our numerical method when applied to (1), in Figures 1 and 2.

Table 2 shows the temporal convergence of the numerical solution to the chosen exact solution, $u = x \exp(-yt)$, of (1). We use the same parameters as

Table 1:

$N \times M$	$\rho = 0.5, r = 0, \mu = 0$				$\rho = 0.9, r = 0.1, \mu = 0.1$			
	E_∞^N	RC	E_2^N	RC	E_∞^N	RC	E_2^N	RC
8x8	1.924e-2	-	5.305e-3	-	3.013e-2	-	8.374e-3	-
16x16	9.917e-3	0.96	1.950e-3	1.44	1.538e-2	0.97	3.039e-3	1.46
32x32	4.995e-3	0.99	7.012e-4	1.48	7.721e-3	0.99	1.086e-3	1.48
64x64	2.502e-3	1.00	2.497e-4	1.49	3.867e-3	1.00	3.864e-4	1.49
128x128	1.252e-3	1.00	9.220e-5	1.44	1.934e-3	1.00	1.424e-4	1.44

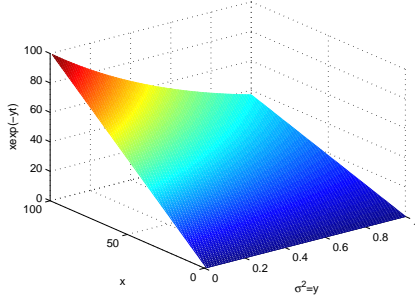


Figure 1: Exact Solution

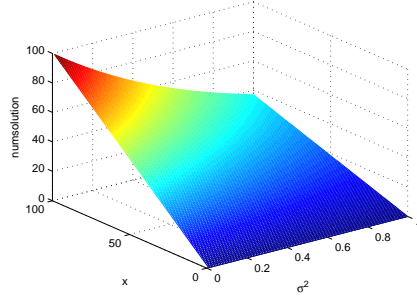


Figure 2: Numerical Solution

in Table 1: $X = Y = T = 1$, $\xi = 1$ and $\zeta = 0.01$. However, the size of the spatial mesh is now fixed to 512×512 as the time step varies. The obtained results show that our numerical method profits from the boundary corrections (25), (27) since it is able to sustain the first order of temporal convergence.

Table 2:

K	$\rho = 0.5, r = 0, \mu = 0$				$\rho = 0.9, r = 0.1, \mu = 0.1$			
	E_∞^N	RC	E_2^N	RC	E_∞^N	RC	E_2^N	RC
16	2.000e-2	-	7.138e-3	-	3.235e-2	-	1.157e-2	-
32	9.859e-3	1.02	3.585e-3	0.99	1.562e-2	1.05	5.753e-3	1.01
64	4.848e-3	1.02	1.796e-3	1.00	7.549e-3	1.05	2.864e-3	1.01
128	2.398e-3	1.02	8.980e-4	1.00	3.721e-3	1.02	1.427e-3	1.01
256	1.197e-3	1.00	4.477e-4	1.00	1.862e-3	1.00	7.099e-4	1.01

The equation (1) degenerates at $x = 0$ and it is well-known that such a behaviour pollutes the numerical solution and deteriorates the accuracy. An effective approach to resolve that issue is application of non-uniform meshes, refined at the area of interest. We present numerical results in Table 3 with an exact solution $u = x \exp(-yt)$ with $K = 1024$ time layers, refining the region of

$x = 0$,

$$\eta_i = i\Delta\eta, \Delta\eta = \frac{1}{M} \sinh^{-1}(X/d), x_i = d \sinh(\eta_i), i = 0, \dots, N$$

where d is a constant ($d = X/700$ in our experiments, h_i^x dominates h_y^j as well as τ), considered in [11, 22]. The mesh refinement is visualized on Figure 3 for $i = 1, \dots, 513$.

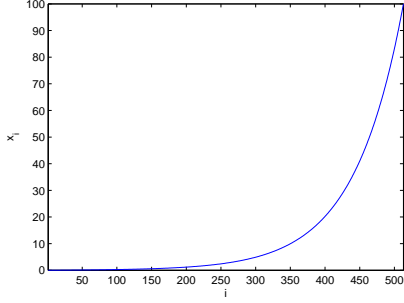


Figure 3: Mesh Refinement $x = 0$

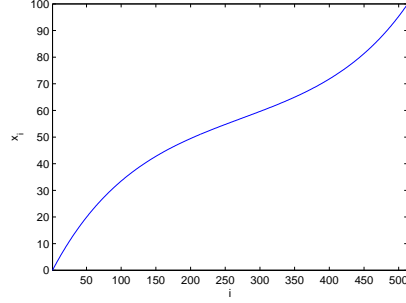


Figure 4: Mesh Refinement $x = E$

Table 3:

$N \times M$	$h_i^x = d(\sinh(\eta_i) - \sinh(\eta_{i-1}))$				$h_i^x = X/N$			
	E_∞^N	RC	E_{RMSE}^N	RC	E_∞^N	RC	E_{RMSE}^N	RC
16x128	2.9859	-	0.1301	-	1.5406	-	0.7970	-
32x128	0.9504	1.65	0.0410	1.67	0.7703	0.99	0.3055	1.38
64x128	0.2640	1.85	0.0122	1.87	0.3851	1.00	0.1159	1.40
128x128	0.0815	1.70	0.0029	1.95	0.1926	1.00	0.0425	1.45

The root mean square error is computed on the region $[0, 0.1X] \times [\zeta, Y]$. One observes improvement of the rate of convergence in both norms when using the discussed non-uniform mesh.

We now solve numerically the original problem $TP1$, characterized by non-smoothness of the terminal (initial) condition (9) on a uniform spatial mesh sized $N \times N$ with $2N$ time layers. In the following Table 4 the mesh C -norm and $RMSE$ -norm are computed w.r.t. the numerical solution on a very fine mesh sized $512 \times 512 \times 1024$. The boundary conditions in direction x are derived by the terminal condition (12). The boundary conditions in direction y are obtained as explained in Section 2, see Figures 5,6. The root mean square error is computed on the region $[0.9E, 1.1E] \times [\zeta, Y]$. The numerical solution of $TP1$ is visualized on Figure 7.

The discontinuity of the terminal (initial) condition characterizes the test problems $TP2$ and $TP3$, seriously deteriorating the accuracy. Table 5 shows

Table 4:

N	8	16	32	64	128	256
E_∞	4.0877	2.0678	0.9911	0.4559	0.1944	0.0649
		(0.983)	(1.061)	(1.120)	(1.230)	(1.584)
E_{RMSE}	0.7641	0.2649	0.1197	0.0551	0.0236	0.0079
		(1.528)	(1.146)	(1.119)	(1.223)	(1.571)

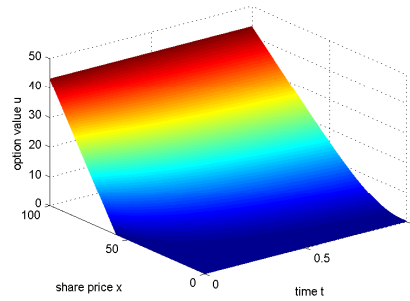
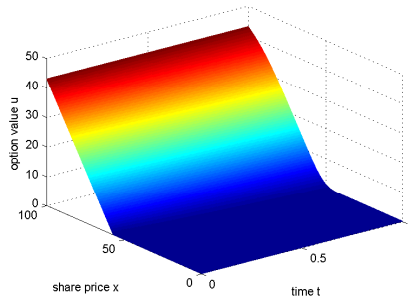


Figure 5: Boundary Condition $y = 0.01$ Figure 6: Boundary Condition $y = Y$

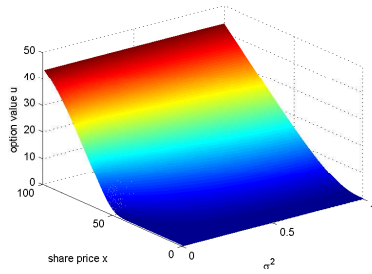


Figure 7: Option Value $TP1$

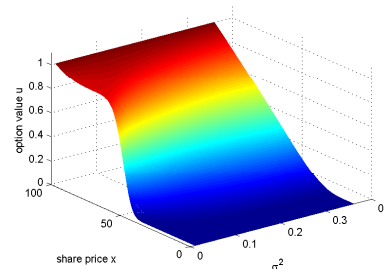


Figure 8: Option Value $TP2$

results for $TP2$ on a non-uniform mesh, refined in the vicinity of $x = E$, and on an uniform mesh. Again, we use the numerical solution on the very fine mesh sized $512 \times 512 \times 1024$ as an exact solution. The mesh size is $N \times N$ with $2N$ time layers and the nodes are generated by the formulas [11, 22] with $c = E/5$, see Figure 4,

$$\eta_i = \sinh^{-1}(-E/c) + i\Delta\eta, \quad \Delta\eta = \frac{1}{N} [\sinh^{-1}((x - E)/c) - \sinh^{-1}(-E/c)],$$

$$x_i = E + c \sinh(\eta_i), \quad i = 0, \dots, N,$$

while the root mean square error is computed on the region $[0.9E, 1.1E] \times [\zeta, Y]$. Again, the boundary conditions in direction y are obtained as explained in Section 2, Figures 9, 10, while the numerical solutions for $TP2$ and $TP3$ are shown on Figures 8, 11 respectively.

Table 5:

N	$h_i^x = c(\sinh(\eta_i) - \sinh(\eta_{i-1}))$				$h_i^x = X/N$			
	E_∞^N	RC	E_{RMSE}^N	RC	E_∞^N	RC	E_{RMSE}^N	RC
32	5.953e-2	-	1.510e-2	-	8.033e-2	-	1.903e-2	-
64	2.642e-2	1.17	7.040e-3	1.10	1.442e-2	2.48	2.412e-3	2.98
128	1.157e-2	1.19	3.044e-3	1.21	1.619e-2	-0.17	6.630e-3	-1.46
256	3.802e-3	1.61	1.018e-3	1.58	5.497e-3	1.56	2.204e-3	1.59

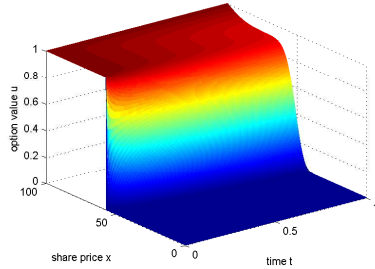


Figure 9: Boundary Condition $y = 0.01$ $TP2$

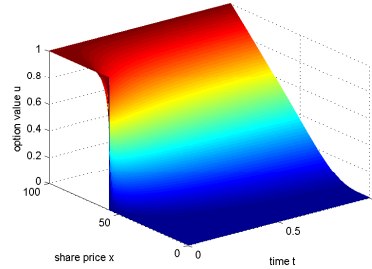


Figure 10: Boundary Condition $y = Y$ $TP2$

We now present numerical experiments for $\zeta = 0$ - a particularly interesting case since one considers degeneration in y -direction. The boundary condition on $y = 0$ is obtained by taking in consideration the deterministic growth of the asset when volatility is zero and therefore we obtain

$$u(x, 0, t) = e^{-rt} u_T(xe^{rt}).$$

It also satisfies the PDE (4) if $y = 0$ and therefore we speak of a *natural boundary condition*. Let us note that one now fixes the non-compatibility of the

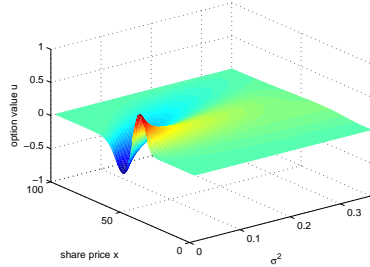


Figure 11: Option Value $TP3$

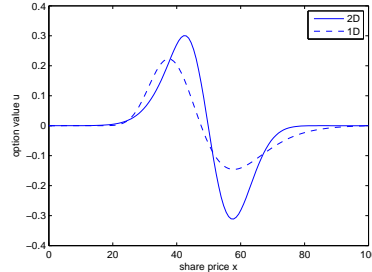


Figure 12: 2D1D $TP3$ $\sigma \approx 0.20$

boundary condition at $x = X$ $u_D(X, y, t) = u_T(X, y)$ with the new boundary condition at $y = 0$ by taking the discount factor into account. We note that the degeneration influences both sub-problems (13),(16). The application of the finite volume method in sub-section 3.3 treats the degeneration in the second sub-problem. The boundary corrections (25), applied to the first sub-problem, have to be computed for $\bar{\alpha}_i = \frac{\bar{b}_{i+1/2}}{\bar{a}_{i+1/2}}$ and therefore we set $\bar{\alpha}_i$ large enough in order to perform the computations since $\bar{a}_{i+1/2} = 0$ if $y = 0$.

Table 6:

N	$8 \times 8 \times 16$	$16 \times 16 \times 32$	$32 \times 32 \times 64$	$64 \times 64 \times 128$	$128 \times 128 \times 256$
E_∞	4.967	2.531 (0.973)	1.180 (1.102)	0.497 (1.248)	0.161 (1.628)
E_{RMSE}	1.066	0.477 (1.160)	0.229 (1.061)	0.101 (1.178)	0.035 (1.545)

Convergence results for the original problem $TP1$ for $\zeta = 0$ w.r.t. the numerical solution on $256 \times 256 \times 512$ are presented in Table 6. We conclude that the numerical method performs well in the case of degeneration in y -direction. The C mesh norm error for $\zeta = 0$, corresponding to Figures 1,2 on a mesh, sized $32 \times 32 \times 64$ is visualized on Figure 13, while the C mesh norm error for $TP1$, $\zeta = 0$ is plot on Figure 14.

In order to show the effects for the variable stochastic volatility we plot the option values of the 2D and 1D simulations, applied to $TP1$ - $TP3$ with and without the stochastic volatility being an independent variable. In the three Figures 12, 15, 16 we see significant differences in those two simulations for fixed values of $\sigma = \sqrt{y}$.

5 Conclusion

In this paper we solve numerically the Hull and White 2D problem (1)-(3) for pricing European options with stochastic volatility, characterized by the

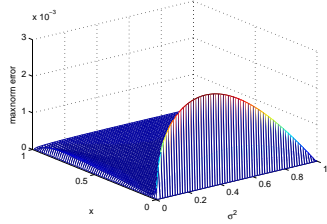


Figure 13: maxnorm error exact solution $32 \times 32 \times 64 \zeta = 0$

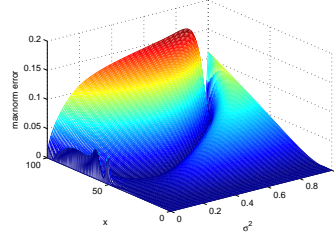


Figure 14: maxnorm error $TP1$ $128 \times 128 \times 256 \zeta = 0$

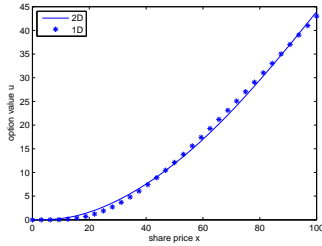


Figure 15: 2D1D $TP1$ $\sigma \approx 0.71$

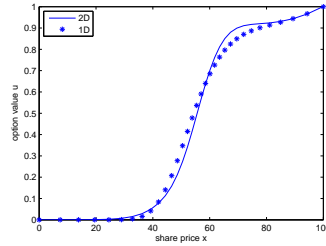


Figure 16: 2D1D $TP2$ $\sigma \approx 0.18$

presence of a mixed derivative term and degeneration on the boundary $x = 0$. The proposed numerical method consists in a LOD operator splitting and a backward Euler semi-discretization in time, while in space a fitted finite volume method is applied. We prove first-order convergence in time. The transition matrices on each time level, resulting from the full discretization, are shown to be M-matrices. The main advantage of the developed numerical method are reduction of the computational costs and non-negativity of the numerical solution in time. Moreover, it produces satisfactory computational results even when degeneration on the boundary $y = 0$ is also considered.

In a forthcoming paper we study the stability and the convergence of the proposed splitting finite volume method.

6 Acknowledgement

The authors would like to thank Prof. Karel in't Hout for his important remarks and suggestions on the differential problem and the numerical method.

The authors are supported by the Sofia University Foundation under Grant No 106/2013. The first author is also supported by the European Social Fund through the Human Resource Development Operational Programme under contract BG051PO001-3.3.06-0052 (2012/2014). The second author is also supported by the Bulgarian National Fund under Project DID 02/37/09.

References

- [1] Y. Achdou, O. Pironneau, Computational Methods for Option Pricing, SIAM in the series Frontiers in Applied Mathematics 2005.
- [2] L. Angermann, Discretization of the Black-Scholes operator with a natural left-hand side boundary condition, Far East J. Appl. Math. 30(1) (2008), pp. 1-41.
- [3] F. Black, M. Scholes, The pricing of options and corporate liabilities, J. Polit. Econ. 81 (1973), pp. 637-659.
- [4] H. Castro, H. Wang, A singular Sturm-Liouville equation under homogeneous boundary condition, Journal of Funct. Anal. 261, 6 (2011) pp. 1542-1590.
- [5] T. Chernogorova, R. Valkov, Finite volume difference scheme for a degenerate parabolic equation in the zero-coupon bond pricing, Math. and Comp. Modeling 54 (2011) pp. 2659-2671.
- [6] T. Chernogorova, R. Valkov, Finite-volume difference scheme for the Black-Scholes equation in stochastic volatility models, Lect. Notes in Comp. Sci. 6046, Springer-Verlag (2011), pp. 377-385.
- [7] C. Clavero, J.C. Jorge, F. Lisbona, Uniformly convergent schemes for singular perturbation problems combining alternating directions and exponential fitting techniques, in: J.J.H. Miller, ed., Applications of Advanced Computational Methods for Boundary and Interior Layers (Boole press, Dublin, 1993) pp. 33-52.
- [8] E.G. D'Yakonov, Difference schemes with splitting operator for multidimensional non-stationary problem, Zh. Vychisl. Mat. i Mat. Fiz. 2 (1962) pp. 549-568.
- [9] D. Gilbarg, N.S. Trudinger, Elliptic Partial Differential Equations of Second Order, 2nd edition, Springer-Verlag 1983.
- [10] T. Gyulov, R. Valkov, Variational formulation for Black-Scholes equation in stochastic volatility models, AIP Conf. Proc. 1497 (2012), pp. 257-264.
- [11] K.J. in't Hout, S. Foulon, ADI finite difference schemes for option pricing in the Heston model with correlation, Int. J. Numer. Anal. Mod. 7 (2010), pp. 303-320.
- [12] C.-S. Huang, C.-H. Hung, S. Wang, A fitted finite volume method for the valuation of options on assets with stochastic volatilities, Computing 77 (2006), pp. 297-332.
- [13] C.-S. Huang, C.-H. Hung, S. Wang, On convergence property of a fitted finite-volume method for the valuation of options on assets with stochastic volatilities, IMA J. Numer. Anal. 30 (2010), pp. 1101-1120.

- [14] W. Hundsdorfer, J. Verwer, Numerical Solution of Time-Dependent Advection-Diffusion-Reaction Equations, Springer-Verlag Berlin Heidelberg 2003.
- [15] J. Hull, A. White, The pricing of options on assets with stochastic volatilities, *J. Fin.* 42 (1987), pp. 281-300.
- [16] S. Ikonen, J. Toivanen, Efficient numerical methods for pricing American options under stochastic volatility, Wiley InterScience 2007.
- [17] A. Kufner, Weighted Sobolev Spaces, New York: John Wiley 1985.
- [18] O.A. Ladyzhenskaja, V.A. Solonnikov, N.N. Ural'tseva, Linear and Quasilinear Equations of Parabolic Type, in: Amer. Math. Soc. Transl. Monographs, Vol. 23 (1968).
- [19] D.W. Peaceman, H.H. Rachford, Jr., The numerical solution of parabolic and elliptic differential equations, *J. Soc. Ind. Appl. Math.* 3 (1955), pp. 28-41.
- [20] A.A. Samarskii, Finite Difference Schemes, Marcel Decker 1992.
- [21] O.A. Oleinik, E.V. Radkevich, Second Order Equations with Nonnegative Characteristic Form, Plenum Press, New York 1973.
- [22] D. Tavella, C. Randall, Pricing Financial instruments, Wiley, New York 2000.
- [23] S. Wang, A novel fitted finite volume method for Black-Sholes equation governing option pricing, *IMA J. Numer. Anal.* 24 (2004), pp. 699-720.
- [24] P. Wilmott, S. Howison, J. Dewynne, The Mathematics of Financial Derivatives, Cambridge University Press, Cambridge 1995.
- [25] N.N. Yanenko, The Method of Fractional Steps, Springer, Berlin 1971.
- [26] Y-l. Zhu, X. Wu, I-L. Chern, Derivative Securities and Difference Methods, Springer, Berlin 2004.
- [27] W. Zhu, D. Kopriva, A spectral element approximation to price European options with one asset and stochastic volatility, *J. Sci. Comput.*, Vol. 42, No. 3 (2010), pp. 426-446.